Investigation of relaxation processes in superfluid ^{3}He-A

Yu. M. Bun'kov, V. V. Dmitriev, and Yu. M. Mukharskiĭ

S. I. Vavilov Institute of Physics Problems, Academy of Sciences of the USSR, Moscow
(Submitted 19 October 1984)
Zh. Eksp.Teor. Fiz. **88**, 1218–1232 (April 1985)

Spin relaxation processes in superfluid ^{3}He-A were investigated by the pulsed NMR methods. At low tilt angles the main relaxation process was that proposed by Leggett and Takagi. When the tilt angle was $\gtrsim 40°$, homogeneous spin precession was unstable and it split into large-amplitude spin waves. In this case the process of relaxation was governed by spin diffusion. A comparison was made of the experimental data with a theory of instability of homogeneous precession suggested by Fomin.

1. INTRODUCTION

Investigations of relaxation processes in superfluid ^{3}He-A by the continuous NMR methods have been made in various laboratories throughout the world[1–4] and they have yielded the NMR line broadening in good agreement with a simultaneously developed theory of "internal" relaxation[5] which takes account of quasiparticle collision processes in ^{3}He-A. However, further investigations of the relaxation processes made by the pulsed NMR methods[6,7] and by the methods involving studies of recovery of the magnetization after an exciting rf pulse with the aid of a SQUID[8,9] have shown that in this case the relaxation processes occur at rates an order of magnitude higher than that predicted by the theory of Leggett and Takagi.[5] The problem of fast spin relaxation in ^{3}He-A (Ref. 10) has been encountered, but this has been solved recently by Fomin[11,12] from the theoretical point of view and in our earlier paper[13] from the experimental point of view. According to Fomin's theory and our experimental data, homogeneous precession in ^{3}He-A is unstable and it splits into large-amplitude spin waves. This destroys the transverse induction signal. A microscopic texture is established and its presence gives rise to strong spin diffusion, so that longitudinal relaxation takes place. We shall give a detailed description of the experiments representing the discovery and investigation of the growth of an instability of homogeneous precession in ^{3}He-A. We shall provide experimental evidence that in the pulsed NMR, under conditions such that an instability does not yet develop, the process of relaxation of ^{3}He-A does occur in accordance with the theory of Leggett and Takagi.

2. APPARATUS

Our experiments were carried out in a cryostat operated on the basis of nuclear demagnetization of copper, cooled first in a dissolution cryostat characterized by a high heat pumping rate. The apparatus was isolated from vibrations by the heavy pendulum method. The apparatus was placed on a base of 800 kg weight suspended by cables 6 m long and had a pneumatic system for raising the apparatus and damping the vibrations. Details of the construction of the apparatus will be described in a paper to be published in "Pribory i tekhnika eksperimenta" and here we shall mention simply the main characteristics. The dissolution cryostat was assembled using four multistage heat exchangers of original construction, which ensured that the heat pumping rate of the cryostat at temperatures 7–30 mK was $100T^4$ (watts). The nuclear stage of the nuclear demagnetization cryostat consisted of 2136 copper wires 0.5 mm in diameter in a glass-fiber insulation. Twelve mols of the copper wire were in the working field of a solenoid[1)] with a critical field 8.9T. The nuclear stage was connected a to a superconducting heat switch composed of 30 lead wires of 99.99 purity and 10 mm length by a heat sink of copper wires 0.5 mm in diameter. The ratio of the resistances at 300 K and 4.2 K for the copper wires in the nuclear stage was 400, whereas for the wires in the heat sink it was 800. A conical junction was used to attach a thermal switch to the dissolution chamber of the cryostat with a solution of ^{3}He in ^{4}He. The total resistance of the conical junction and of the heat sink was 0.8 $\mu\Omega$ at 4.2 K. The working chamber was attached to the cover of the nuclear stage by the conical junction and was located in the region of compensation of the field of the main solenoid. The necessary magnetic field was created by an additional solenoid which also had gradient coils either for creation or for compensation of a magnetic field gradient in the region of the working chamber. The general appearance of the chamber is shown in Fig. 1. A sintered heat exchanger made of a silver powder with grain size ~ 100 nm and total area $\sim 10 \text{m}^2$ was located in the lower part of the chamber. The upper demountable part of the chamber consisted of a copper cover attached to the lower copper part by copper bolts and isolated hermetically by an indium seal, and of a working part made of Stycast 1266 epoxy resin. The thermal resistance between liquid ^{3}He placed in the working chamber and the nuclear demagnetization stage was $1000/T$ (K/W). The sensitive element of an NMR thermometer of the PLM-3 type, a heater, and two containers for the study of the NMR of ^{3}He were placed inside the working chamber.

The dissolution cryostat cooled the nuclear stage to ~ 16 mK. After demagnetization it was possible to investigate superfluid ^{3}He for periods up to 12 days. The lowest temperature of ^{3}He reached by us was 0.6 mK and it was governed by the small size of the heat exchanger, but the relatively high thermal resistance between ^{3}He and the nuclear stage made it possible to maintain the necessary ^{3}He

 0038-5646/85/040719-09$04.00

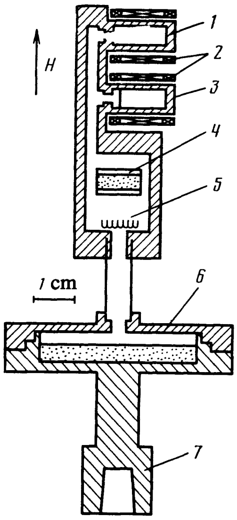

FIG. 1. Schematic diagram of the working chamber: 1) chamber for investigating ^3He in the open geometry; 2) sectioned rf coils; 3) chamber with a set of Dacron plates; 4) NMR thermometer sensor; 5) heater; 6) chamber with sintered silver heat exchanger; 7) conical junction to a nuclear demagnetization cryostat.

temperature by dissipating a small amount of heat in the heater. One of the containers for the study of the NMR of ^3He was a cylinder 5 mm in diameter and 13 mm long which was connected through a narrow passage to the rest of ^3He. The second container was a $5\times5\times12$ mm parallelepiped and it was filled with Dacron plates 0.01 mm^2 thick and separated by distances 0.3 mm. In some of the experiments these plates were oriented at right-angles to the external magnetic field, whereas in others they were oriented along this field. The ^3He in the chamber was under a pressure of 29.3 bar. The experiments were carried out in a magnetic field corresponding, in the range of small tilt angles, to the ^3He-A precession frequencies of 250 and 500 kHz. In the first experiments the rf coils were wound directly on the working chamber. However, it was found that then in ~ 10 msec from an rf pulse a thermal wave traveled in ^3He. Next, rf coils were suspended so that they were not in contact with the working chamber, and thermal contact with the chamber of dissolution of ^3He in ^4He of the dissolution cryostat was provided by four copper wires bonded into the body of the coil. The rf coils were used to excite ^3He with an rf magnetic field and to detect the nuclear induction signal. They were in the form of a solenoid of 15 mm length and 9 mm in diameter and they were wound in three sections in order to improve the homogeneity of the rf field throughout the sample. With the same idea in mind the ^3He container inside the working chamber was closed by a stopper with an aperture for heat exchange. The distribution of the rf field and of the amount of ^3He along the chamber axis was determined (Fig. 2). The rf field distribution was monitored by a probe receiving coil 1 mm in diameter and then it was adjusted by altering the number of the copper wires in the outer sections of the coil. Such careful measures for the control of the rf field were needed because the NMR precession frequency of ^3He-A depended on the angle of tilt of the megnetization and, consequently, an inhomogeneity of the rf field resulted in dephasing of the induction signal.

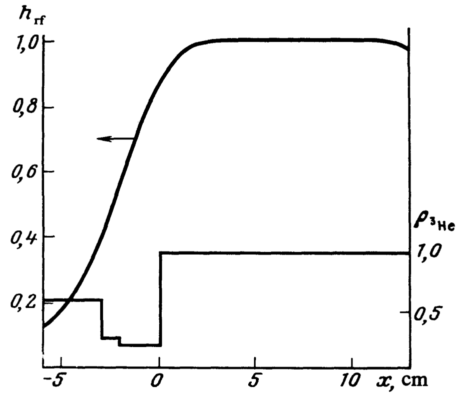

FIG. 2. Distribution of the amplitude h_{rf} of the rf field along the axis of the working chambers and the distribution of the amount of ^3He, denoted by $\rho_{^3He}$, in a chamber without plates.

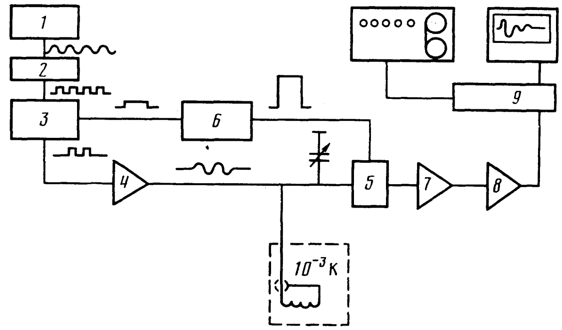

FIG. 3. Block diagram of an NMR spectrometer: 1) reference oscillator; 2) modulator; 3) logic device; 4) resonance amplifier; 5) active damper; 6) damper control circuit; 7) preamplifier; 8) resonance amplifier; 9) digital memory.

The NMR spectrometer was specially prepared for the experiments on ^3He. It was distinguished by a high power which made it possible to tilt the magnetization of ^3He by 90° in four oscillation periods at a frequency of 250 kHz. The spectrometer will be described in detail in a separate communication, but here we shall provide a brief account of its construction. A block diagram of the spectrometer is shown in Fig. 3. A sinusoidal signal from a reference oscillator was applied to a modulator, where it was converted into a square wave matched to the input of TTL logic circuits. The logic unit created a train of pulses with a selected number of oscillations and a period double that of the reference signal. An rf pulse was amplified in a class C resonance power amplifier. This circuit ensured a good isolation of the receiving system from the transmitter noise and doubling of the period had the advantage that in the absence of the rf pulses at the power amplifying input there was no signal at the working frequency. The power amplifier created a field up to 12 Oe in the receiving-transmitting coil.

The receiving part of the NMR spectrometer consisted of a wide-band preamplifier with a gain of 100 and a resonance amplifier tuned to a frequency of 250 or 500 kHz. The width of the pass band of the amplifier was 20 kHz. The

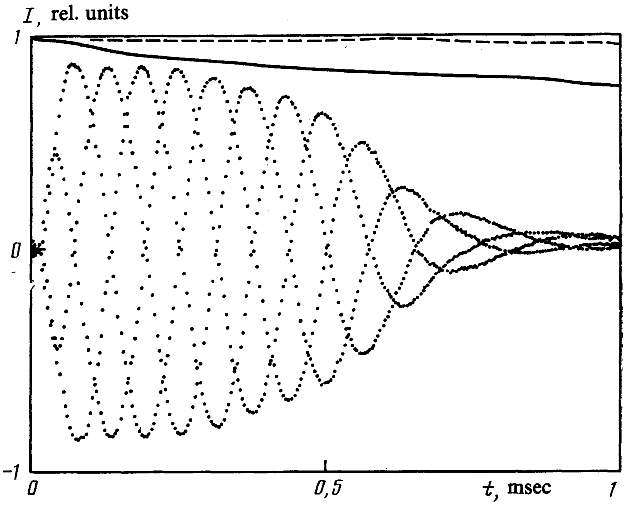

FIG. 4. Record of an induction signal exhibited by ^{3}He-A after an 81° magnetization tilt. The separation between the points is 1 μsec. The curves represent the decay of the free induction signal of the normal phase of ^{3}He at the frequency of 250 kHz, representing homogeneity of the external magnetic field (dashed curve) and decay of the ^{3}He induction signal (continuous curve) because of inhomogeneity of the exciting rf field, calculated for the conditions under which the experimental record was obtained.

"ringing" time of the input circuit was reduced and the preamplifier saturation was prevented by placing in front of the latter an active controlled damper assembled from MOS transistors, which reduced an rf pulse of 100 V amplitude tot he microvolt level at the receiver input. The use of this damper and the fairly wide band of the resonance amplifier shortened the dead time of the receiving system to 60 μsec at frequencies 250 and 500 kHz.

After passing through the amplifiers, the induction signal was stored in digital form in a Datalab-905 storage device; this was done at 1024 points with the maximum recording frequency 5 MHz; the final stage was an analysis on a computer. The recording frequency was usually selected to be close to four times the signal frequency, which reduced the errors in the determination of the frequency and amplitude of the induction signal. When the signal had to be observed over more than 256 periods, a suitable separation between the points was selected so that the signal at the neighboring points changed in phase by $\sim\pi/2 + 2n\pi$.

3. INVESTIGATIONS OF THE FREE INDUCTION SIGNAL IN ^{3}He-A

The modern rf spectroscopic technique for NMR and homogeneous external and rf fields enabled us to discover that the induction signal of ^{3}He-A had an unusual form and it also varied with the frequency. The first experiments were carried out as follows. An external field was selected so that a tilt of the magnetization by an angle of 7° did not affect the phase of the induction signal at the recording points, i.e., the recording frequency was a multiple of the frequency of the induction signal. In the limit of small angles, it is found that in the case of ^{3}He-A

$$\omega_0^2=\gamma^2H^2+\Omega_A^2, \tag{1}$$

where ω_0 is the induction signal frequency; γ is the gyromagnetic ratio for ^{3}He; Ω_A is the frequency that represents the shift of the NMR frequency in ^{3}He-A and is of dipole-dipole origin.[15] The resonance magnetic field intensity was used to find Ω_A and the known dependence $\Omega_A(T)$ was employed to obtain the temperature. Moreover, the NMR frequency in ^{3}He-A depended on the angle β of the magnetization tilt away from the external magnetic field[16]:

$$\omega_\perp^2=\gamma^2H^2+\Omega_A^2(^1/_4+^3/_4\cos\beta). \tag{2}$$

The angle of tilt of the magnetization of ^{3}He by an rf pulse was calibrated using the induction signal for the normal phase. According to a computer calculation of the motion of the magnetization under the action of our rf fields,[13] a change in the angle of tilt because of a frequency shift in the A phase relative to calibration was less than 2° for the maximum value of Ω_A and tilt angles $\sim 100°$. Figure 4 shows a typical record of an induction signal obtained for the magnetization tilted at 81°($\omega_0 = 250$ kHz; $\Omega_A = 55$ kHz). It is clear that the phase of the recorded signal varies with time, indicating that the induction frequency is different from 250 kHz; it is also clear that the frequency of the induction signal varies with time. We used the computer to approximate each 16 points by a sinusoid of suitable frequency, phase, and amplitude and in this way we restored the characteristics of the initial induction pulse and either displayed them on a screen or used a plotter. An analysis of the frequency dependence of the NMR signal on the angle of tilt of the spins gives results which agree well with Ref. 16. The change in the frequency of the induction signal with time carries, as shown below, information on the relaxation of the tilt angle of the spins β, and on the formation of macroscopic spin waves.

It is clear from the record shown in Fig. 4 that the induction signal decayed in 0.8 msec when the magnetization was tilted by 81°. Such a rapid fall of the signal could not be explained by an inhomogeneity of the external field or of the rf field or by the process of "internal" relaxation. Figure 4 shows also the decay of the induction signal in the same field observed in the normal phase of ^{3}He. This decay is a measure of the inhomogeneity of the external field. Dephasing of the induction signal in ^{3}He-A because of the inhomogeneity of the rf field was calculated on a computer for given tilt angles and temperatures, in accordance with the distribution of the rf field and of ^{3}He in the chamber (Fig. 2), which is also shown in Fig. 4. We can see that both these "external" dephasing processes represent a small fraction of the decay of the induction signal. The natural decay of the induction signal in ^{3}He can be determined more accurately by eliminating dephasing because of inhomogeneities of the external and rf fields.

The time dependences of the intensity of the induction signal obtained for different tilt angles at a temperature $T = 0.93T_c$ and frequency 250 kHz are collected in Fig. 5. The experimental dependences are represented by points. The continuous curves show the fall of the induction signal in the case of spatially homogeneous relaxation. The theoretical curves in Fig. 5 are calculated using a formula suggested by Fomin[17]:

$$du/dt=2\varkappa(\Omega_A/4)^4(1-u)(35u^3+55u^2+25u+13), \tag{3}$$

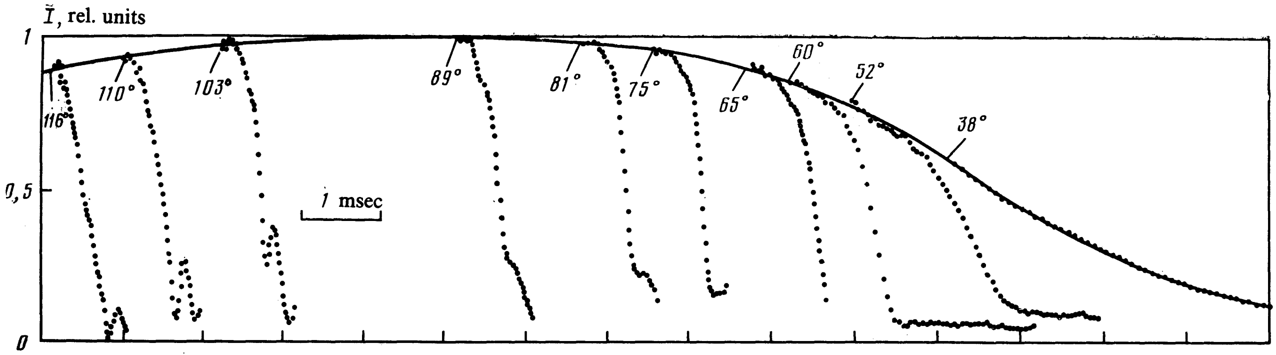

FIG. 5. Decay of the ^{3}He-A induction signal observed for different angles of tilt of the magnetization (points). The continuous curve is the decay of the induction signal predicted by the theory of Leggett and Takagi under homogeneous relaxation conditions. The beginning of each experimental dependence is made to fit the theoretical curve in accordance with the tilt angle ($\omega_0 = 250$ kHz, $\Omega_A = 55$ kHz).

where $u = \cos\beta$ and φ is a phenomenological parameter. The quantity φ can be obtained quite easily as follows. The dependence (3) in the range of small β has the asymptote

$$(1-u)=(1-u_0)\exp\{-\varkappa\Omega_A{}^4(t-t_0)\}, \tag{4}$$

whereas according to the theory of Leggett and Takagi the broadening of the NMR line of ^{3}He-A is[18]

$$\frac{1}{T_\perp}=\frac{1-\lambda}{2\lambda}\frac{\Omega_A{}^4}{\gamma^2H^2+\Omega_A{}^2}\tau\left(1+\frac{z_0}{4}\right)^{-1}, \tag{5}$$

which gives

$$\varkappa=\frac{1-\lambda}{\lambda}\tau\gamma^{-2}H^{-2}\left(1+\frac{z_0}{4}\right)^{-1}. \tag{6}$$

In these expressions the notation is as follows: λ is the ratio of the magnetic moment of the superfluid part of ^{3}He to the total magnetic moment; z_0 is the Fermi liquid correction describing the deviation of the susceptibility of the normal component of ^{3}He from the ideal Fermi gas; τ is the quasiparticle collision time in superfluid ^{3}He, which is the main parameter characterizing the process of "internal" relaxation of Leggett and Takagi. In the derivation of Eq. (6) it is assumed that for small angles of spin tilt the Leggett-Takagi relaxation mechanism is found to be the dominant one, in agreement with the results of our experiments. The theoretical curve in Fig. 5 was described by us using the value $\tau T_c^2 = 0.29$ mK$^2\cdot\mu$sec, where T_c is the temperature of the phase transition of ^{3}He to the phase A at a given pressure. This value of τ differs somewhat from the value obtained using the continuous NMR data,[4] but they do agree well with the acoustic experiments[19] and with our data. The quantities λ and z_0 are also taken from the review of Ref. 19.

The theoretical curve in Fig. 5 shows the dependence of the transverse magnetization of ^{3}He-A on time $S_\perp(t) = S_0\sin[\beta(t)]$, in accordance with the theory of Leggett and Takagi for a specific experimental situation. In comparing this curve with the experimental data the initial point of the experimental dependence, obtained for different tilt angles β_0, is made to match the same angle of tilt on the theoretical curve and the subsequent behavior of the angle β_0 is studied on the same time scale. It is quite clear that for tilt angles of $\lesssim 38°$ the transverse magnetization of ^{3}He-A relaxes in good agreement with the theory of Leggett and Takagi. In the case of large tilt angles there are additional processes that result in a much faster change in the transverse magnetization.

We carried out a similar comparison for the time dependence of the induction signal frequency (Fig. 6). The theoretical curve was taken to be $\omega_\perp[\beta(t)]$, obtained from Eq. (2) and from the same dependence $\beta(t)$ as in the preceding case. The experimental points were made to match the theoretical curve in respect of the initial spin tilt. We can also see that for spin tilt angles in the range $\lesssim 52°$ the precession frequency follows the theoretical curve. In the case of large angles of tilt

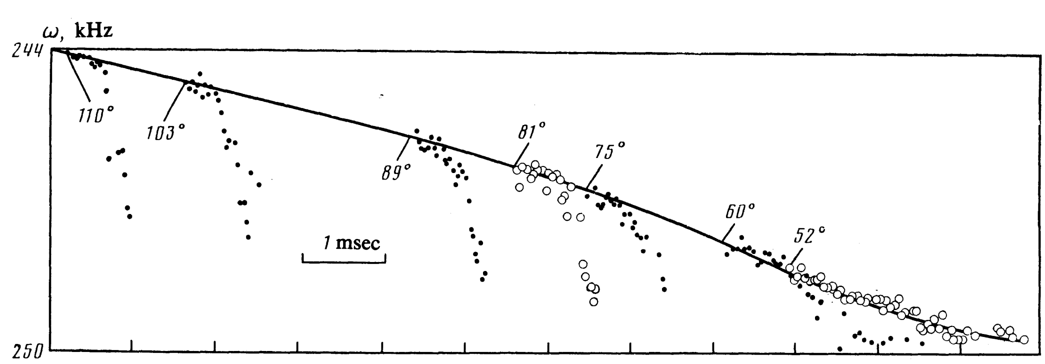

FIG. 6. Time dependences of the frequency of the induction signal observed for different tilts of the magnetization (●, ○). The continuous curve is the time dependence of the frequency of the induction signal in the case of homogeneous relaxation in accordance with the theory of Leggett and Takagi. The beginning of each experimental dependence is made to fit the theoretical curve in accordance with the tilt angle ($\omega_0 = 250$ kHz, $\Omega_A = 55$ kHz).

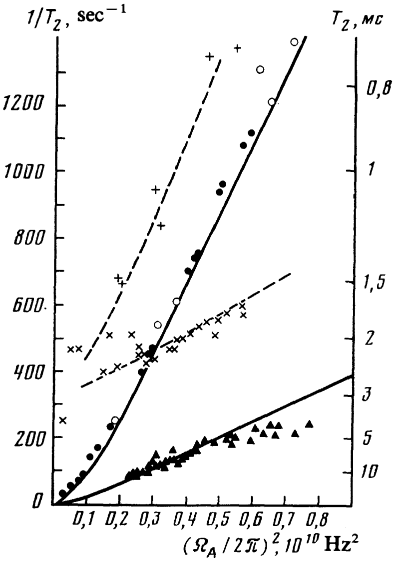

FIG. 7. Dependences of the decay decrement of the induction signal for magnetization tilt angles $\lesssim 20°$ on Ω_A^2, obtained for NMR frequencies 250 kHz (●, ○, +) and 500 kHz (▲, ×) in an open geometry chamber containing ^{3}He-A (●, ▲) and in a chamber with plane-parallel plates oriented parallel to the magnetic field (○) and across the magnetic field (+, ×). The continuous curves are the dependences predicted by the theory of Leggett and Takagi on the assumption that $\tau T_c^2 = 0.29\,\mu\text{sec}\cdot(\text{mK})^2$.

of the magnetization the frequency of precession is reestablished much faster than would follow from the theory of Leggett and Takagi. It should be pointed out that if in the case of an investigation of the amplitude of the induction signal we obtain information on the change in the transverse magnetization of ^{3}He-A, averaged over the size of the chamber, then an investigation of the induction signal frequency can give data on the average angle of tilt of the magnetization, naturally when ^{3}He-A is assumed to be homogeneous. Knowing the angle of tilt of the magnetization and its transverse component, we can then determine the dependence of the change in the total magnetization of ^{3}He-A averaged over the whole sample. (The external causes of dephasing are small and are allowed for in the analysis.) It is found that for tilt angles of $\lesssim 38°$ the total magnetization of ^{3}He is conserved. For higher tilt angles the total magnetization falls in approximately the same way as the transverse magnetization, since a change in the angle β (and in the frequency) lags in time after changes in the transverse magnetization and hence we may conclude that the spatial homogeneity of the precession in ^{3}He-A is greatly disturbed.

4. INVESTIGATIONS OF RELAXATION OF ^{3}He-A IN THE HOMOGENEOUS RANGE

The range of angles of tilt of the magnetization of ^{3}He-A in which the homogeneity of a sample does not become disturbed in the available time during the relaxation process depends strongly on temperature. However, for angles of $\lesssim 25°$, we find that liquid ^{3}He remains homogeneous during relaxation throughout the range of existence of ^{3}He-A in the investigated magnetic fields. For tilt angles less than 20° the process of relaxation of the transverse magnetization in ^{3}He-A is exponential and, therefore, it can be described by a damping decrement $1/T_2$. Figure 7 shows the experimental values of the damping decrement of the induction signal plotted as a function of Ω_A^2 and, consequently, as a function of temperature at NMR frequencies 250 and 500 kHz; the open circles represent the damping decrement of the induction signal in a chamber with Dacron partitions oriented parallel to the magnetic field. These results are in satisfactory agreement with those obtained for free ^{3}He. Figure 7 includes the theoretical dependences deduced from the theory of Leggett and Takagi in accordance with Eq. (5), assuming that τ is 4.6×10^{-8} sec, which (as pointed out in the preceding section) are in agreement with the acoustic data. The dependence of the quantity

$$\frac{1-\lambda}{\lambda}\left(1+\frac{1}{4}z_0\right)^{-1}$$

on Ω_A is obtained by a suitable conversion of the curve given in the review of Wheatley (Fig. 27 in Ref. 19).

It follows from the experimental data that relaxation in the chamber with a set of plates parallel to the external field occurs at the same rate as in the chamber containing free ^{3}He. The situation changes drastically if the same plates are oriented at right-angles to the external magnetic field. The experimental results for the damping decrement of the induction signal obtained for this case are represented by crosses in Fig. 7. It is quite clear that in addition to the Leggett-Takagi relaxation mechanism, there is another practically additive mechanism resulting in an additional increase of the damping decrement which is practically independent of temperature and of the field intensity. The origin of this additional relaxation mechanism is not yet clear.

5. INVESTIGATIONS OF THE PROCESS OF DEVELOPMENT OF AN INSTABILITY OF HOMOGENEOUS PRECESSION

The behavior of the nuclear induction signal obtained for ^{3}He-A in the case of large tilt angles of the nuclear magnetization is in good agreement with the ideas of an instability of homogeneous precession of ^{3}He-A and its decay into large-amplitude spin waves. This process was predicted theoretically by Fomin in 1979 (Ref. 11). Our experiments stimulated Fomin to investigate theoretically the influence of this process on the experimentally observed amplitude and frequency of the induction signal.[12] According to the formalism developed by Fomin, if the magnetic field is sufficiently strong so that $\gamma H \gg \Omega_A$, we can use the Leggett equations of motion averaged with respect to time $t \gg (\gamma H)^{-1}$ and $t \ll (\Omega_A)^{-1}$. The motion of the magnetization of ^{3}He-A is described by four variables: the magnetization S, its angle of tilt β from the magnetic field, the phase of precession α, and the angle Φ governing the relative phase of the precession and rotation of the spin part of the order parameter about S, and it has a solution describing precession of the magnetization at a frequency $\omega_\perp(\cos\beta)$ when $S = S_0 = \text{const}$, $\beta = \beta_0 = \text{const}$, $\alpha = \alpha(t) = \omega t + \text{const}$, $\Phi = 0$. A solution of linearized equations of motion for small spatial perturbations of the homogeneous precession is[11]

$$\cos\beta = \cos\beta_0 + \varepsilon(r),\quad \alpha = \alpha_0 + \nu(r),\quad S = S_0 + \sigma(r),$$
$$\Phi = \Phi_0 + \Psi(r)$$

if we allow for the gradient energy and spin diffusion. It has the form of spin waves

$$\varepsilon, \nu, \Psi=\varepsilon_0, \nu_0, \Psi_0\cdot\exp(i\omega_k t-ikr), \quad (7)$$

$$\omega_k=\left\{\frac{C_{kk}}{4\gamma^2H^2}\left(C_{kk}-\frac{3}{4}\Omega_A^2\sin^2\beta\right)\right.$$
$$\left.\times\frac{\Omega_A^2(3-\cos\beta)(1+\cos\beta)+4C_{kk}}{\Omega_A^2(1+\cos\beta)^2+4C_{kk}}\right\}^{1/2}-iD_{kk}, \quad (8)$$

where $C_{kk}=C_{\alpha\beta}{}^2k_\alpha k_\beta$; $D_{kk}=D_{\xi\eta}k_\xi k_\eta$; $C^2_{\alpha\beta}$ is the tensor of the squares of the spin wave velocities; $D_{\xi\eta}$ is the tensor of the spin diffusion coefficients.

In the limit of the spin system ^{3}He-A at rest, for $\sin\beta=0$ and for perturbations ε, ν, and Ψ we can have solutions in the form of traveling spin waves which are damped out by spin diffusion.

In the case of a spin system tilted at an angle from H, the frequency of oscillations of spatial inhomogeneities with a wave vector k satisfying the condition $C_{\alpha\beta}{}^2k_\alpha k_\beta<\frac{3}{4}\Omega_A{}^2\sin^2\beta$, is purely imaginary and a solution of the equations of motion for perturbations has the form of an exponentially rising function

$$\varepsilon, \nu, \Psi=\varepsilon_0, \nu_0, \Psi_0\cdot\exp\{\Gamma_k t-ikr\}, \quad (9)$$

where $\Gamma_k=|\omega_k|$. Therefore, against the background of homogeneous precession, a spatial inhomogeneity with a growth increment Γ_k develops. The magnitudes of the perturbations ε, ν, and Ψ are found to be of the same order of magnitude, whereas σ is considerably less. A qualitative representation of a given oscillation mode can be found in Fig. 8. It is known that during precession of the magnetization S around H the vector of the order parameter d moves on a path similar to the figure eight (see Ref. 10). The spatial orientation of the phase Φ coincides with a node of this path.

The influence of growing inhomogeneities on the experimentally observed amplitude and frequency of the free induction signal can be determined by a suitable calculation and integration with respect to all values of k. It should be borne in mind that, in general, the initial perturbations ε_0, ν_0, and Ψ_0 also depend on k and the problem becomes very complex.

If the initial perturbations have the same sufficiently small amplitudes for all values of k (for example, if they are thermal fluctuations), then using the circumstance that Γ_k has a maximum Γ_m in its dependence on k it can be shown—as is done in Ref. 12—that the experimentally observed transverse magnetization and precession frequency should have the following time dependences:

$$\langle S_\perp\rangle=S_{\perp0}\left[1-\frac{A_S}{(2\Gamma_m t)^{1/2}}\exp(2\Gamma_m t)\right], \quad (10)$$

$$\left\langle\frac{d\alpha}{dt}+1+\frac{3}{8}\frac{\Omega_A^2}{\gamma H}(1+\cos\beta)\right\rangle=\frac{A_\delta}{(2\Gamma_m t)^{1/2}}\exp(2\Gamma_m t), \quad (11)$$

where A_S and A_δ are constants corresponding to the initial perturbations of the system. If, for the sake of simplicity, we shall assume that $C^2_{\alpha\beta}$ is proportional to $D_{\alpha\beta}$, then Γ_m can be written in the form[12]

$$\Gamma_m=\frac{3}{16}\frac{\Omega_A^2}{\gamma H}K_m\sin^2\beta, \quad (12)$$

where K_m is the maximum (in the dependence on z) value of the function

$$K_z=2\left\{z(z-1)\frac{2+3zu+u}{2+3zu-u}-\Lambda z\right\}, \quad (13)$$

where

$$\Lambda=2\omega D_{\alpha\beta}/C_{\alpha\beta}^2;\quad u=1-\cos\beta;\quad z={}^4/_3C_{kk}\Omega_A^{-2}\sin^{-2}\beta. \quad (14)$$

Therefore, on condition of a uniform (with respect to k) initial distribution of perturbations, experimental results should manifest inhomogeneities with the largest growth increment. Then, the existence of inhomogeneities with other values of k gives rise to a factor $(2\Gamma_m t)^{1/2}$ in Eqs. (10) and (11), but in the range of times $t\gg 1/\Gamma_m$ this factor is a smooth function and changes only the normalization of the initial perturbation of the system represented by A_S.

In our first experiments[13] we found that the induction signal of ^{3}He-A obtained for magnetization tilt angles $\gtrsim 40°$ decreases in accordance with the law

$$I=I_0(1-A_S\exp t/T_\Phi). \quad (15)$$

It was also shown there that the quantity T_Φ^{-1} depends on the temperature, magnetic field, and tilt angle β in the same way as $2\Gamma_m$, but the former is several times smaller than predicted theoretically by Fomin.

We carried out a more detailed investigation of the induction signal in order to find the reason for the quantitative discrepancy between the theoretical and experimental val-

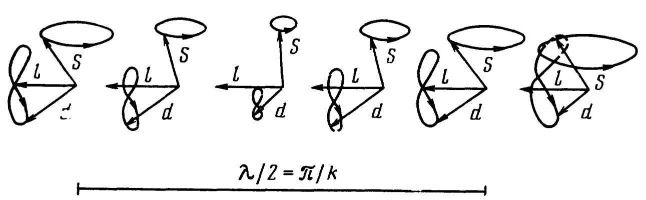

FIG. 8. Spatial distribution of the phase and amplitude of precession and of the angle Φ in the case of growth of a spatial inhomogeneity with a wave vector k.

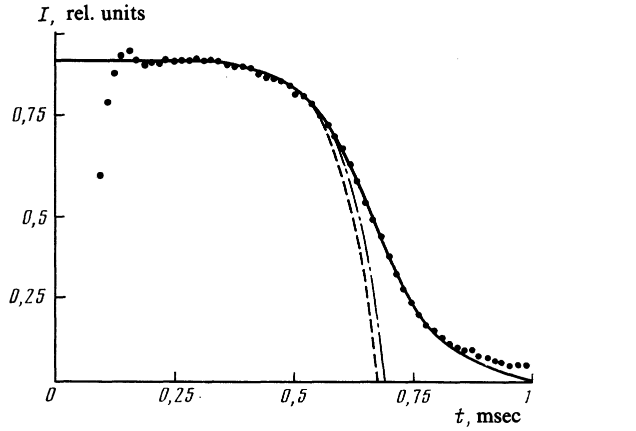

FIG. 9. Decay of the ^{3}He-A induction signal for the magnetization tilt angle 81° ($\omega_0=250$ kHz, $\Omega_A=55$ kHz). The dashed curve is the dependence (10), the chain curve is the dependence (15), and the continuous curve represents Eq. (16). For all these dependences it is assumed that $T_\Phi=75\ \mu$sec.

ues of the quantity referred to above. Special attention was concentrated on the fact that the fall of the induction signal intensity is best described by the function

$$I=I_0(1+A_S\exp t/T_\Phi)^{-1}, \tag{16}$$

which in the range $A_S\exp(t/T_\Phi)\ll 1$, i.e., during the initial stage of the development of the instability when Fomin's theory is valid, is identical with Eqs. (10) and (15). On the other hand, the dependence (16) reflects the circumstance that the growth of an instability whould be limited. Figure 9 shows a comparison of the dependences such as the Eqs. (10), (15), and (16) with an experimental induction decay curve obtained for $\beta_0 = 81°$, $\omega_0 = 250$ kHz, and $\Omega_A = 55$ kHz. For all these curves we found that $T_\Phi = 75$ μsec.

The induction decay curve was then described by the values of A_S and T_Ψ selected on a computer in such a way that the rms deviation of the experimental points from the dependence (16) was minimized in the region of the fall of the intensity of the induction signal to half its initial value. This procedure reduced the random scatter in the determination of A_S and T_Φ.

The main conflict between Fomin's theory and our experimental results is the observation that the initial perturbations represented by the experimental dependences are within the range 10^{-3}–10^{-5}, whereas an inhomogeneity due to thermal fluctuations was estimated by Fomin to be 10^{-7}. Another source of inhomogeneity is a texture arising from the presence of the chamber walls. Its magnitude is of the order of $\delta/a \approx 10^{-3}$ (where δ is the magnetic length and a is the length of the chamber along the magnetic field) for $k\sim 2\pi/a \sim 10\ \mathrm{cm}^{-1}$ and it decreases on increase in k. We can see that, under the experimental conditions, the first to grow is an instability with a wave vector smaller than the optimal value $[k_{\mathrm{opt}} \approx (3/8)^{1/2}\Omega_A \sin\beta/C_{\alpha\beta} \approx 10^3]$ and, consequently, with a smaller growth increment, but a much larger value of the initial inhomogeneity. This is supported indirectly by the results obtained for the induction signal in the chamber with plates. The characteristics of the induction signal for the chamber with plates oriented along the magnetic field are practically the same as in the chamber without plates, whereas in the chamber with plates across the magnetic field an instability develops much faster.

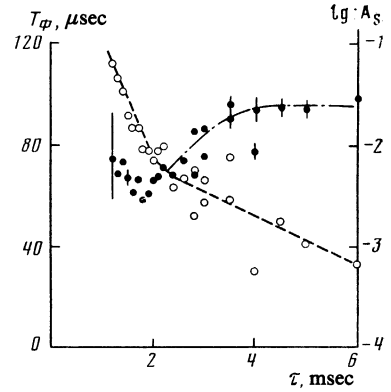

FIG. 11. Dependences of the time constant of the growth of an instability (●) and of the initial value of the inhomogeneity A_S (○) after a 90° pulse on the delay time τ from a 90° prepulse ($\omega_0 = 500$ kHz, $\Omega_A = 66$ kHz).

A more detailed confirmation of the hypothesis that the initial inhomogeneities are distributed nonuniformly with respect to k was provided by the following series of experiments carried out in the working chamber.

It is natural to expect that after decay of the induction signal the relative magnitude of the inhomogeneities with high values of Γ_k is considerably greater than in an equilibrium situation. Therefore, if after a certain delay time following the first pulse a second rf pulse is applied, the decay of the induction signal should proceed at a rate characterized by a higher value of $1/T_\Phi$. Our experimental investigation fully confirmed this hypothesis. Figure 10 shows a series of experimental induction decay curves after a 90° rf pulse which followed, after various delays, a 90° prepulse. Figure 11 shows the dependences of the observed quantities T_Φ and A_S on the delay time. We can see that when the delay is ~ 2 msec, the value of T_Φ has a definite minimum which coincides with the end of the induction signal due to the prepulse

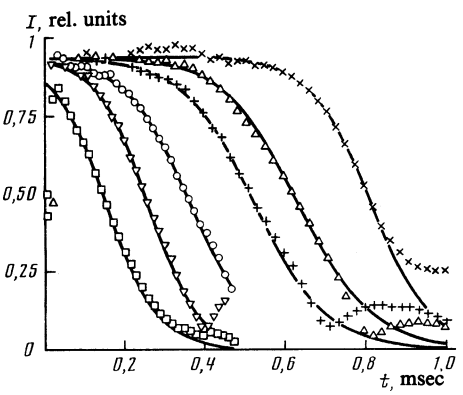

FIG. 10. Experimental induction decay curves obtained for a 90° rf pulse applied after a time t from a 90° prepulse: $t = \infty$ (×); 6 msec (△); 4.5 msec (+); 2.8 msec (○); 2 msec (▽); 1.5 msec (□). The curves represent the results of an analysis of the experimental dependences on a computer ($\omega_0 = 500$ kHz, $\Omega_A = 66$ kHz).

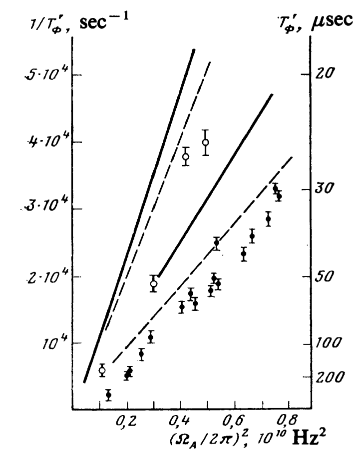

FIG. 12. Dependences of the maximum growth increment of an inhomogeneity $1/T_{\Phi'}$ on Ω_A^2 at the frequency of 500 kHz for $\beta = 90°$ (●) and at the frequency of 250 kHz for $\beta = 81°$ (○). The continuous curves are the theoretical dependences (12) calculated for $\Lambda = 0$, $\omega_0 = 250$ kHz, $\beta = 81°$, and for $\Lambda = 0$, $\omega_0 = 500$ kHz, $\beta = 90°$; the dashed curves correspond to $\Lambda = 0.25$, $\omega_0 = 250$ kHz, $\beta = 81°$ and $\Lambda = 0.5$, $\omega_0 = 500$ kHz, $\beta = 90°$.

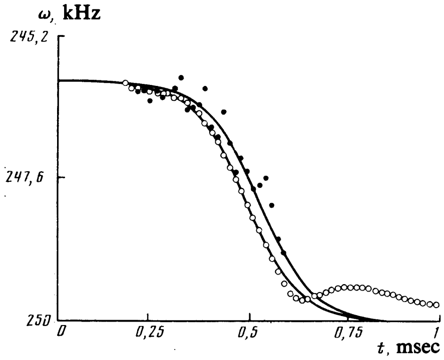

FIG. 13. Comparison of the decay of the induction signal (○) and of the change in the frequency of the induction signal (●) with time ($\omega_0 = 250$ kHz, $\beta = 81°$, $\Omega_A = 55$ kHz). A prepulse was used in order to ensure a higher precision of the results.

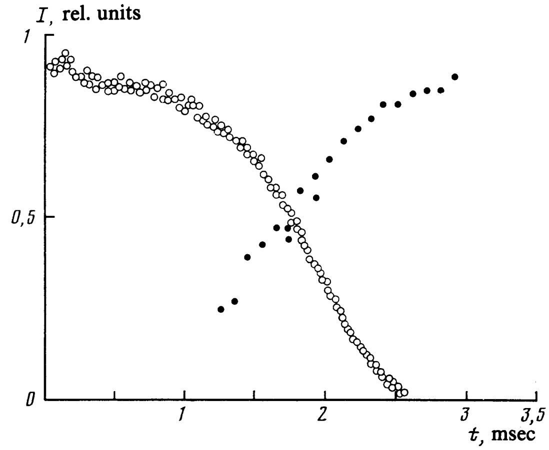

FIG. 14. Decay of the induction signal in a homogeneous field (○) and recovery of the longitudinal magnetization observed by a two-pulse method in an inhomogeneous field (●) under the same experimental conditions ($\omega_0 = 500$ kHz, $T = 0.966T_c$).

and which can be associated with the maximum relative growth of instabilities characterized by the largest values of Γ_k. An increase in T_Φ after long delays is due to the fact that the inhomogeneities with large values of k relax faster because of spin diffusion.

Therefore, in Fomin's theory it is more natural to compare $2\Gamma_m$ with $1/T_{\Phi'}$ obtained at the minimum of the dependences of the type shown in Fig. 11. A comparison of the value of $1/T_{\Phi'}$ with Fomin's theory is made in Fig. 12 for NMR frequencies 250 and 500 kHz. It is quite clear that $1/T_{\Phi'}$ is quantitatively close to the theoretical value $2\Gamma_m$. Unfortunately, we cannot say that $1/T_{\Phi'}$ corresponds to the maximum growth increment of the inhomogeneities and, therefore, these data cannot be used to find the value of $\Lambda = 2\omega D/c^2$, but we can say that it does not exceed 0.7 for $\omega = 500$ kHz and we can thus obtain an estimate of the diffusion coefficient in ^{3}He-A given by $D/c^2 \lesssim 0.7$ (MHz)$^{-1}$. According to Fomin's theoretical estimates given in Ref. 12, we should have $D/c^2 \approx 0.5$ (MHz)$^{-1}$.

We also investigated the time dependence of the frequency of the induction signal, which was found to be the same as the time dependence of the induction signal intensity. A comparison is made in Fig. 13 between the experimental time dependences of the intensity (amplitude) and frequency of the induction signal for the magnetization tilt angle 61° at 250 kHz. We can see that the constant T_Φ is the same for both dependences and that A_δ, depending on the induction signal frequency, is somewhat smaller than A_S, which is in qualitative agreement with Fomin's theory. In fact, dephasing of homogeneous precession produces a texture and it simultaneously results in diffusion relaxation of the magnetization. These two effects reduce the shift of the induction signal frequency relative to the equilibrium value. On the other hand, the decay of the shift of the induction signal frequency lags behind dephasing, because of a reduction in the total intensity.

We tested whether the investigated mechanism of instability of homogeneous precession did indeed govern the processes of longitudinal relaxation in ^{3}He-A by comparing the process of decay of homogeneous precession with the process of recovery of the longitudinal magnetization determined by a two-pulse method of the kind used in Refs. 6 and 7. A spin system exposed to a strongly inhomogeneous magnetic field was subjected to a 90° pulse and then, after a delay time, to a 7° probe pulse. The intensity of the induction signal after the 7° pulse could be used to determine the degree of recovery of the longitudinal magnetization. It was found that this method could be used only at very high temperatures, because at lower temperatures the form of the induction signal after a 7° pulse depended strongly on the delay time. Figure 14 compares the process of decay of the induction signal intensity in a homogeneous field with recovery of the magnetization in an inhomogeneous field. Clearly, the time scale of the two processes is the same.

6. CONCLUSIONS

The good quantitative agreement between the experimental results and the theory of instability of homogeneous precession demonstrates that such precession in ^{3}He-A decays into large-amplitude spin waves when the magnetization tilt angle is large. Under real experimental conditions the texture singularities may result in nucleation of spin waves at the walls of the chamber and then the spin waves travel into the interior of the chamber. A departure from the spatial homogeneity of spin precession of ^{3}He-A activates spin-diffusion relaxation mechanisms and these ensure rapid relaxation of the nuclear magnetization.

Another interesting result of our investigation is the observation of a slow relaxation of the quantity A after the action of a prepulse. In other words, in the case of ^{3}He-A there is a mechanism which ensures that the spatial inhomogeneity is retained for a fairly long time. This mechanism is clearly a perturbation of the texture of the vector representing the orbital momentum l. In fact, in a coherent spin wave shown in Fig. 9 the homogeneity of the average direction of the vector d is disturbed and, because of the spin-orbit coupling, this should result in a breakdown of the homogeneity of the vector l. In view of the large viscosity, the orbital system of ^{3}He-A clearly retains the spatial inhomogeneity over periods of ~ 10 msec.

It is very interesting to investigate an instability of homogeneous precession in rotating ^{3}He-A, in which there is a texture of vortices with a characteristic size dependent on the rotation velocity. The dependence of T_Φ on the rotation velocity may make it possible to match the diffusion coefficient D, the velocity of spin waves c, and the distance between vortices.

It would be interesting to carry out experiments on effects of acoustic excitation on the instability of homogeneous precession. However, in the range $k \sim 10^3$ cm^{-1} an acoustic wave is strongly damped and this complicates experiments.

In conclusion, we wish to express our deep gratitude to A. S. Borovik-Romanov, whose direction of this investigation has largely ensured its successful completion, and to I. A. Fomin who influenced greatly our work by his theoretical investigations and by numerous discussions. We are also grateful to S. M. Elagin for the assembly and operation of the ultralow temperature apparatus.

[1)] This solenoid was developed and made at the I. V. Kurchatov Institute of Atomic Energy in Moscow.[14]

[1]H. M. Bozler, M. E. R. Bernier, W. J. Gully, R. C. Richardson, and D. M. Lee, Phys. Rev. Lett. **32**, 875 (1974).

[2]D. D. Osheroff, S. Engelsberg, W.F. Brinkman, and L. R. Corruccini, Phys. Rev. Lett. **34**, 190 (1975).

[3]O. Avenel, M. E. Bernier, E. J. Varoquaux, and C. Vibet, Proc. Fourteenth Intern. Conf. on Low-Temperature Physics, Otaniemi, Finland, 1975 (ed. by M. Kruisius and M. Vuorio), Vol. 5, North-Holland, Amsterdam, 1975, p. 429.

[4]W. J. Gully, C. M. Gould, R.C.Richardson, and D. M. Lee, J. Low Temp. Phys. **24**, 563 (1976).

[5]A. J. Leggett and S. Takagi, Phys. Rev. Lett. **34**, 1424 (1975).

[6]L. R.Corruccini and D. D. Osheroff, Phys. Rev. B **17**, 126 (1975).

[7]R.W.Giannetta, E. N. Smith, and D. M. Lee, J. Low Temp. Phys. **45**, 295 (1981).

[8]R.A. Webb, Phys. Rev. Lett. **40**, 883 (1978).

[9]R. E. Sager, R. L. Kleinberg, P. A. Warkentin, and J. C. Wheatley, J. Low Temp. Phys. **32**, 263 (1978).

[10]D. M. Lee and R. C. Richardson, in: The Physics of Liquid and Solid Helium (ed. by K. H. Bennemann and J. B. Ketterson), Part II, Wiley, New York, 1979, p. 287.

[11]I. A. Fomin, Pis'ma Zh. Eksp. Teor. Fiz. **30**, 179 (1979) [JETP Lett. **30**, 164 (1979)].

[12]I. A. Fomin, Pis'ma Zh. Eksp. Teor. Fiz. **39**, 387 (1984) [JETP Lett. **39**, 466 (1984)].

[13]A. S. Borovik-Romanov, Yu. M. Bun'kov, V. V. Dmitriev, and Yu. M. Mukharskiĭ, Pis'ma Zh. Eksp. Teor. Fiz. **39**, 390 (1984) [JETP Lett. **39**, 469 (1984)].

[14]O. P. Anashkin, V. E. Keilin, M. I. Surin and V. Kh. Shleifman, Cryogenics **19**, 405 (1979).

[15]D. D. Osheroff, W. J. Gully, R. C. Richardson, and D. M. Lee, Phys. Rev. Lett. **29**, 920 (1972).

[16]D. D. Osheroff and L. R. Corruccini, Phys. Lett. A **51**, 447 (1975).

[17]I. A. Fomin, Zh. Eksp. Teor. Fiz. **77**, 279 (1979) [Sov. Phys. JETP **50**, 144 (1979)].

[18]A. Abragam and M. Goldman, Nuclear Magnetism: Order and Disorder, Clarendon Press, Oxford, 1982 [Russ. Transl., Mir, M., 1984].

[19]J. C.Wheatley, in: Progress in Low Temperature Physics (ed. by D. F. Brewer), Vol. VIIA, North-Holland, Amsterdam, 1978, p. 1.

Translated by A. Tybulewicz